

Cardiac Functional Analysis by Free-Breath Real-Time Cine CMR with a Spatiotemporal Filtering Method, TSENSE: Comparison with Breath-Hold Cine CMR

Masaki Yamamuro, MD,¹ Eiji Tadamura, MD, PhD,² Shotaro Kanao, MD,¹ Satoshi Okayama, MD,² Jun Okamoto, PhD,³ Shinichi Urayama, PhD,⁴ Takeshi Kimura, MD, PhD,⁵ Masashi Komeda, MD, PhD,⁶ Toru Kita, MD, PhD,⁵ and Kaori Togashi, MD, PhD¹

Department of Diagnostic Imaging and Nuclear Medicine, Kyoto University Graduate School of Medicine, Kyoto, Japan¹

First Department of Internal Medicine, Nara Medical University, Nara, Japan²

MR Business Management Group, Medical Solutions, Marketing Division, Siemens-Asahi Medical Technologies Ltd.³

Human Brain Research Center, Kyoto University Graduate School of Medicine, Kyoto, Japan⁴

Department of Cardiovascular Medicine, Kyoto University Graduate School of Medicine, Kyoto, Japan⁵

Department of Cardiovascular Surgery, Kyoto University Graduate School of Medicine, Kyoto, Japan⁶

ABSTRACT

The aim of this study was to assess the accuracy of cardiac functional values obtained from free-breathing real-time cine CMR with the temporal sensitivity encoding (TSENSE) technique by comparing them with values obtained from conventional cine CMR. For the real-time cine CMR, two protocols were employed, one with good temporal resolution and one with good spatial resolution. The functional values obtained from the high temporal resolution real-time cine CMR agreed and correlated well with those of cine CMR. On the other hand, statistically significant but clinically slight overestimation of ESV ($p < .05$) and underestimation of EF ($p < .01$) were observed with the other protocol. Real-time cine CMR with TSENSE can provide acceptable cardiac functional values.

INTRODUCTION

Cardiac functional analysis is important in the treatment of coronary artery disease. To date, cardiac magnetic resonance imaging (CMR) has been a reference standard in the measurement of left ventricular (LV) volume and mass because it is independent of geometric assumptions, is noninvasive, and is free of exposure to contrast agents or radiation (1–3). Also of note, real-time cine CMR can provide cardiac functional images without breath holding (4–6).

A spatiotemporal filtering method, TSENSE (a Works-in-Progress sequence, Siemens, Erlangen, Germany) has recently

been introduced to real-time cine CMR to achieve image reconstruction with better absolute temporal resolution (7). TSENSE combines temporally interleaved k-space lines to generate coil sensitivity maps directly from imaging data. A sliding window method is used to update the coil sensitivity estimation for every phase, but the raw data for each reconstructed image is unique, that is, each raw data point is used in only one reconstruction. As a result, both faster data acquisition and higher true, not effective, temporal resolution of reconstructed images are achieved (Fig. 1).

However, validation of the volume measurements has not been completed yet. Thus, the aim of this study was to assess the accuracy of global cardiac functional values obtained from free-breathing real-time cine CMR with TSENSE, by comparing with values obtained from breath-hold cine CMR.

MATERIALS AND METHOD

Twenty-two patients diagnosed with coronary artery disease underwent cardiac CMR from August 2004 to April 2005. The study group consisted of 14 men (age range, 46–84 years; mean age, 68 years) and 8 women (age range, 54–83 years; mean age, 67 years). Mean heart rate during the acquisition of CMR ranged from 51 to 98 beats per minute (mean \pm standard deviation,

Received 12 July 2005; accepted 11 April 2006.

Keywords: Cardiac Function, CMR, Real-Time

Correspondence to:

Masaki Yamamuro, MD

Department of Diagnostic Imaging and Nuclear Medicine,

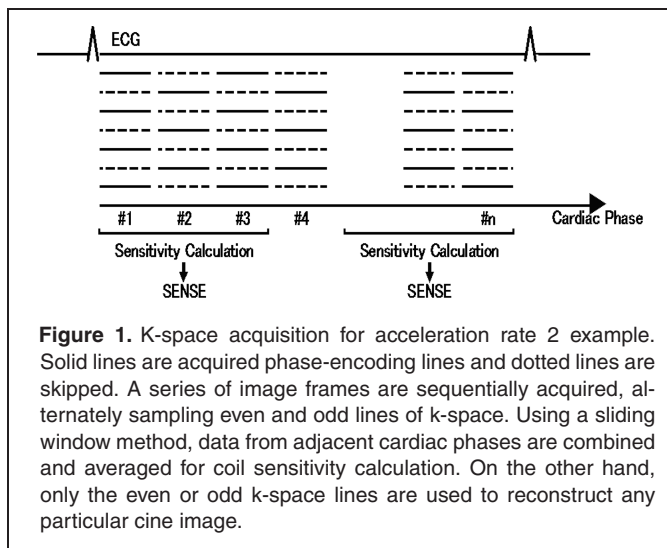
Kyoto University Graduate School of Medicine,

54 Shogoinkawahara, Sakyo-ku,

Kyoto, 606-8507, Japan

fax: 81-75-751-3217

email: myamamu@kuhp.kyoto-u.ac.jp



69 ± 11). A total of 11 patients had myocardial infarction, and 11 had angina pectoris. All patients were referred for cardiac CMR for clinical reasons, and informed consent to participate in our study was obtained from each. Our institutional review board approved this study.

CMR was performed on a 1.5T whole-body imager (Symphony; Siemens, Erlangen, Germany) with multiple surface coils connected to phased-array receivers. Free-breathing real-time cine CMR was acquired using a work-in-progress cine CMR application with TSENSE. The patients were told to breathe shallowly during the data acquisition (1). Two different protocols, one with good temporal resolution (protocol A, temporal resolution ~60 ms) and one with good spatial and worse temporal resolution (protocol B, temporal resolution ~90 ms) were applied. Imaging parameters of protocol A were as follows: repetition time/echo time, 2.2/1.1 ms; flip angle, 55°; acceleration factor, 3; matrix, 74_128; and field of view, 340_340. Imaging parameters of protocol B were as follows: repetition time/echo time, 2.6/1.3 ms; flip angle, 55°; acceleration factor, 3; matrix, 86_192; and field of view, 340_340. Breath-hold cine CMR (temporal resolution ~60 ms) was acquired using a segmented true FISP (fast imaging with steady-state precession) sequence (8-11). Imaging parameters were as follows: repetition time/echo time, 3.6/1.8 ms; flip angle, 60°; 13 lines per segment; matrix, 208_256; and field of view, 340_340. To acquire three-dimensional LV data in each of the cine CMR studies, magnetic resonance (MR) images of 9–13 contiguous sections with a thickness of 8-mm and an interslice gap of 2 mm were obtained in the short-axis plane, covering the entire left ventricle from the base to the apex (2). Imaging parameters of the three cine CMR protocols are summarized in Table 1.

MR images were analyzed by an experienced observer without any other clinical information, but with the aid of commercially available software (Argus; Siemens). Image analysis was followed by manual delineation of the LV border. As previously described, papillary muscles were regarded as being part of the LV cavity (2,12). Subsequently, end-diastolic volume (EDV) and

Table 1. Three Cine CMR Protocols

	Real-Time CMR (Protocol A)	Real-Time CMR (Protocol B)	Segmented true FISP CMR
TR (ms)	2.2	2.6	3.6
TE (ms)	1.1	1.3	1.8
Flip angle (°)	55	55	60
Lines per segments	n.a.	n.a.	13
Acceleration factor	3	3	n.a.
Temporal Resolution (ms)	66.4	92.8	46.8
Field of View (mm)	340 × 340	340 × 340	340 × 340
Acquisition Matrix	74 × 128	86 × 192	208 × 256
Spatial Resolution	3.5 × 2.7	3.0 × 1.8	1.6 × 1.3
Slice thickness (mm)	8	8	8
Interslice gap (mm)	2	2	2

FISP = fast imaging with steady-state precession.

end-systolic volume (ESV), and LV mass were calculated on the basis of the Simpson rule. LV mass was calculated as the product of the myocardium specific gravity (i.e., 1.05 g/cm³) and the integrated LV myocardial area (2,12). Finally, the EF was calculated from the EDV and ESV values (2,12). Additionally, interobserver variability was tested by comparing measurements obtained by two experienced observers.

Statistical Analysis

The functional values obtained from the two free-breathing real-time cine CMR protocols were compared to those from the breath-hold cine CMR, the reference standard. Systemic error and the degree of agreement of various functional values based on free-breathing and breath-hold cine CMR were assessed according to the method described by Bland and Altman (13). The degree of agreement between the two methods was expressed as the mean difference (bias), standard deviation of the differences, limits of agreement (mean ± 2 standard deviation), standard error of the mean difference, and the 95% confidence interval of the mean difference. A one-sample *t* test was used to determine whether the resulting difference from zero, as an under- or overestimation with real-time cine CMR, was significant. In a second analysis, linear regression was used to compare the functional values obtained from free-breathing real-time cine CMR and from breath-hold cine CMR. A *p* value of less than .05 was assumed to indicate statistical significance.

RESULTS

Result values are expressed as mean ± standard deviation.

Both real-time imaging techniques (protocols A and B) yielded high-quality images, allowing the assessment of ventricular volume and mass (Fig. 2). The data acquisition time for both real-time CMR protocols was significantly shorter than that for the breath-hold cine CMR (8.2 ± 1.1 sec for protocol A, 9.1 ± 1.2 sec for protocol B, and 10.4 ± .3.1 min for cine CMR, *p* < .001).

A summary of the data obtained with each of the three cine CMR protocols is presented in Table 2. The results of the

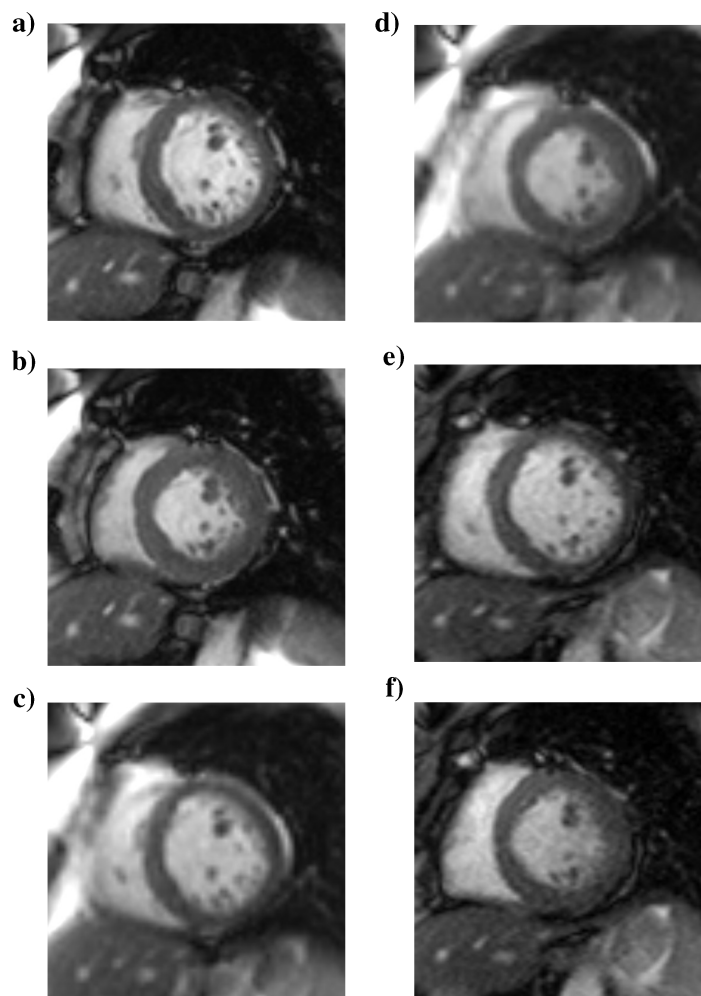


Figure 2. End-diastolic and end-systolic short-axis images in a patient with angina pectoris obtained by each cine CMR technique are presented. (a) A typical end-diastolic short-axis image by true FISP cine CMR. (b) A corresponding end-systolic short-axis image by true FISP cine CMR. (c) A typical end-diastolic short-axis image by real-time cine CMR with TSENSE with protocol A. (d) A corresponding end-systolic short-axis image by real-time cine CMR with TSENSE with protocol A. (e) A typical end-diastolic short-axis image real-time cine CMR with TSENSE with protocol B. (f) A corresponding end-systolic short-axis image by real-time cine CMR with TSENSE with protocol B. Both real-time imaging techniques yielded good-quality images, allowing the assessment of ventricular volume and mass.

Table 2. Functional Values Obtained from Each Cine CMR Protocol

	LVEF (%)	EDV (mL)	ESV (mL)	LV mass (g)
Real-time CMR (Protocol A)	41.2 ± 17.0	164.0 ± 64.8	104.4 ± 66.0	137.5 ± 42.7
Range	11 ~ 71	68 ~ 336	27 ~ 299	75 ~ 263
p value	0.40	0.97	0.98	0.53
Real-time CMR (Protocol B)	39.6 ± 16.7	164.0 ± 66.0	108.1 ± 69.0	139.0 ± 41.5
Range	8 ~ 65	75 ~ 327	27 ~ 302	68 ~ 274
p value	<.01	0.97	<.05	0.14
segmented true FISP CMR	42.0 ± 17.2	164.1 ± 65.7	104.4 ± 68.7	135.9 ± 42.5
Range	10 ~ 69	66 ~ 343	20 ~ 308	60 ~ 268

EDV = end-diastolic volume, EF = ejection fraction, ESV = end-systolic volume, FISP = fast imaging with steady-state precession, LV = left ventricular.

Bland-Altman analysis are shown in Table 3 and Fig. 3. The Bland-Altman analysis revealed no significant degree of directional measurement bias when data obtained with protocol A were compared with those of breath-hold cine CMR. No significant difference of the mean difference from 0 was found for any parameter. On the other hand, significant overestimation of ESV ($p < .05$) and underestimation of EF ($p < .01$) were observed with protocol B. Results of the linear regression analysis are shown in Table 4. The various functional values obtained with both real-time cine CMR protocols were closely correlated with the values obtained from breath-hold cine CMR.

An interobserver variability of 8.9% for EF, 7.8% for EDV, 9.7% for ESV and 11.6% for LV mass was found with Protocol A, and an interobserver variability of 6.9% for EF, 7.5% for EDV, 8.0% for ESV and 9.1% for LV mass was found with Protocol B. On the other hand, an interobserver variability of 6.6% for

Table 3. Results of the Bland-Altman Analysis

	LVEF (%)	EDV (mL)	ESV (mL)	LV mass (g)
Real-time CMR (Protocol A)				
Bias ± SD	-0.8 ± 4.3	-0.1 ± 11.2	0.1 ± 8.6	1.6 ± 11.5
Limits of agreement (2SD)	8.6	22.3	17.2	23.0
95% Confidence interval	1.8	4.7	3.6	4.8
SE of the mean difference	0.9	2.4	1.8	2.5
Regression line	$y = -0.01 \times -0.3$	$y = -0.01 \times +2.2$	$y = -0.04 \times +4.2$	$y = 0.004 \times +0.9$
p value	0.40	0.97	0.98	0.53
Real-time CMR (Protocol B)				
Bias ± SD	-2.4 ± 3.0	-0.1 ± 12.2	3.7 ± 7.9	3.0 ± 9.1
Limits of agreement (2SD)	6.1	24.3	15.9	18.3
95% Confidence interval	1.2	5.1	3.3	3.8
SE of the mean difference	0.7	2.6	1.7	1.9
Regression line	$y = -0.03 \times -1.2$	$y = 0.004 \times -0.8$	$y = -0.006 \times +3.1$	$y = 0.02 \times +6.4$
p value	<.01	0.97	<.05	0.14

For protocol A, no significant degree of directional measurement bias was observed in any of the comparisons of real-time cine CMR and breath-hold true FISP cine CMR data. No significant difference of the mean difference from 0 was found for any parameter in protocol A. For protocol B on the other hand, Bland-Altman analysis revealed significant overestimation of ESV ($P < .05$) and underestimation of EF ($P < .01$) when compared with breath-hold true FISP cine CMR. EDV = end-diastolic volume, EF = ejection fraction, ESV = end-systolic volume, FISP = fast imaging with steady-state precession, LV = left ventricular.

EF, 7.2% for EDV, 8.2% for ESV and 8.9% for LV mass was found with breath-hold cine CMR.

DISCUSSION

Our study showed that free-breathing real-time cine CMR with the TSENSE technique is capable of providing accurate global cardiac functional values. Our study also indicated that temporal resolution was important for cardiac functional evaluation.

Temporal resolution is an important factor for accurate measurement of cardiac volumes (11,14). The absolute temporal resolution of real-time CMR without TSENSE is approximately 180 msec, insufficient for the precise analysis of cardiac function (4). Therefore, echo-sharing techniques have been a necessity; namely, images were reconstructed from several in-

terleaved spiral trajectories in k-space after applying a sliding window method (4). As a result, effective temporal resolution, defined as the time interval between successive reconstructed temporal-phase images, was increased to 90 msec or less (4,15,16). Lee et al. showed that measurements of resting left-ventricular function via real-time CMR with an effective temporal resolution of ~90 msec were comparable to those derived from a series of separate breath-hold single-section true FISP acquisitions (15). Controversially, Barkhausen et al. indicated that an effective temporal resolution of ~75 msec lead to overestimation of ESV and underestimation of EF when using both techniques (14). Kaji et al. reported that evaluation of LV volume and mass was feasible without breath-holding by applying real-time CMR with an effective temporal resolution of ~60 msec (4). They also recommended better *absolute* temporal resolution to further improve measurement fidelity (4). Recently, a spatiotemporal filtering method, TSENSE, was introduced

Table 4. Results of the Linear Regression Analysis

	LVEF (%)	EDV (mL)	ESV (mL)	LV mass (g)
Real-time CMR (Protocol A)				
Correlation coefficient (r)	0.97	0.99	0.99	0.96
SEE	4.4	11.6	8.4	12.0
Regression line	$y = 0.96 \times +1.0$	$y = 0.97 \times +4.5$	$y = 0.95 \times +4.9$	$y = 0.97 \times +5.9$
Real-time CMR (Protocol B)				
Correlation coefficient (r)	0.98	0.98	0.99	0.98
SEE	3.1	12.7	8.3	9.4
Regression line	$y = 0.96 \times -0.5$	$y = 0.99 \times +2.1$	$y = 0.99 \times +3.8$	$y = 0.95 \times +9.4$

The various functional data obtained from both real-time cine CMR protocols were closely correlated with those obtained from breath-hold cine CMR. EDV = end-diastolic volume, EF = ejection fraction, ESV = end-systolic volume, FISP = fast imaging with steady-state precession, LV = left ventricular.

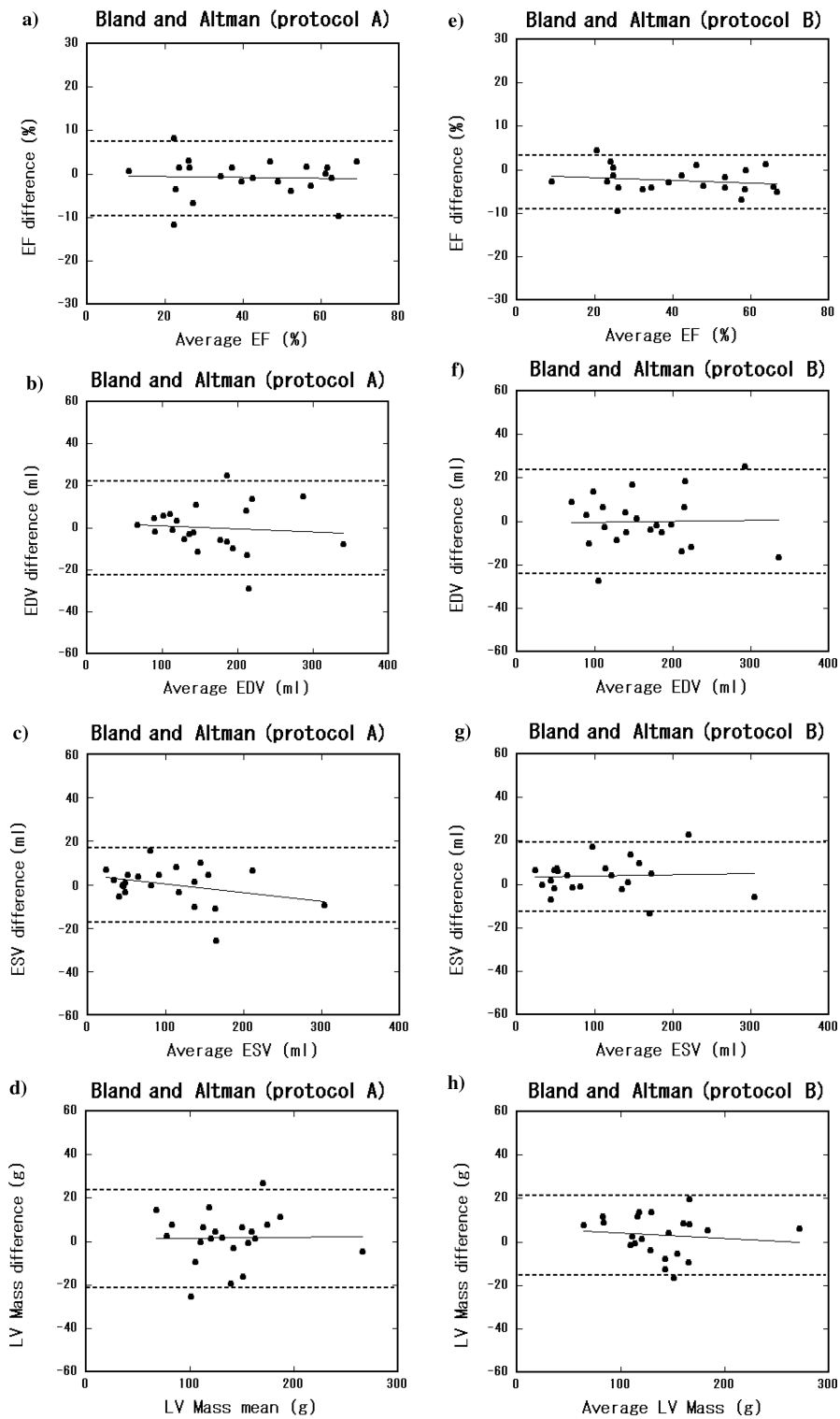


Figure 3. The Results of the Bland-Altman Analysis. Bland and Altman analysis of (a) LVEF, (b) EDV, (c) ESV and (d) LV mass by real-time cine CMR with TSENSE with protocol A and true FISP cine CMR or Bland and Altman analysis of (e) LVEF, (f) EDV, (g) ESV and (h) LV mass by real-time cine CMR with TSENSE with protocol B and true FISP cine CMR. Bland-Altman analysis revealed significant overestimation of ESV ($P < .05$) and underestimation of EF ($P < .01$) in free-breath real-time cine CMR with protocol B compared with breath-hold true FISP cine CMR. On the other hand, no significant degree of directional measurement bias was observed in any of the comparisons of real-time cine CMR with protocol A and breath-hold true FISP cine CMR data. No significant difference of the mean difference from 0 was found for any parameter in protocol A. EDV = end-diastolic volume, EF = ejection fraction, ESV = end-systolic volume, FISP = fast imaging with steady-state precession, LV = left ventricular.

to real-time cine CMR to achieve higher absolute temporal resolution (7). Therefore, we compared various functional values obtained from real-time cine CMR (absolute temporal resolution of ~60 msec and ~90 msec) with those from true FISP cine CMR.

In the current study, the various functional data obtained via the real-time cine CMR protocol with better temporal resolution (~60 msec) were closely correlated and agreed well with those obtained from breath-hold cine CMR. On the other hand, slight but significant overestimation of ESV and underestimation of EF were observed with the higher spatial-resolution protocol (worse temporal resolution, ~90 msec). Thus, for accurate cardiac functional evaluation, temporal resolution was found to be more important than spatial resolution. In a previous study, Miller, et al. also suggested that ESV and EF were affected mainly by changes in the temporal resolution rather than the spatial resolution (11). In addition, Lee, et al. suggested that their aforementioned study (temporal resolution of ~90 msec) was limited to the measurement of resting LV function in a sample of patients with heart rates that ranged from 55 to 90 bpm, and, at higher heart rates, the accuracy of measurements (particularly ESV and consequently EF) would diminish unless further improvements in temporal resolution could be achieved (15). However, the sample size of our current study was small. In addition, the bias \pm SD even in protocol B might be too slight to have clinical significance. Although a larger group of subjects would possibly increase statistical significance, such a difference might not necessarily imply clinical significance.

On the other hand, the spatial resolution of real-time CMR, less than that of conventional cine CMR, has been considered a limitation (4,17). The real-time CMR protocol with ~60 ms temporal resolution had a spatial resolution of $3.5 \times 2.7 \text{ mm}^2$ versus $1.5 \times 1.3 \text{ mm}^2$ for the true FISP cine CMR protocol. In general, the decrease in spatial resolution might decrease the accuracy for the delineation of the end- and epicardial borders of LV. However, considering the good agreement between functional measurements obtained with real-time and cine CMR, the current spatial resolution of real-time CMR is acceptable for quantitative analysis of global cardiac function. Also of note, zero filling was applied in both real-time CMR protocols to make better use of k-space information, and to reduce partial-volume effects and edge-detection artifacts.

The comparison to another sequence is also an important issue. Compared to integrated parallel acquisition techniques (iPAT), TSENSE provides two potential advantages: faster acquisition by deriving coil sensitivity maps from the acquired data, rather than from additionally sampled central k-space lines; and a more robust coil sensitivity estimation by temporal filtering of the data and more available k-space information (18). When compared to echo-sharing, or temporal interpolation, TSENSE offers the advantage of reconstructing images with true temporal resolution. The temporal resolution of the coil sensitivity map is lowered by averaging data across several frames, but the image data used for reconstruction is not shared or interpo-

lated. However, the comparison of various functional values obtained from TSENSE to those from another technique was not performed in the present study. Therefore, the present studies did not directly indicate the superiority of TSENSE to another technique in cardiac functional analysis.

CONCLUSION

Free-breathing real-time cine CMR with TSENSE was capable of providing accurate cardiac functional values when a protocol with sufficient absolute temporal resolution was applied.

REFERENCES

1. Higgins CB. Which standard has the gold? (editorial). *J Am Coll Cardiol* 1992;19:1608–1609.
2. Pattynama PM, Lamb HJ, van der Velde EA, van der Wall EE, de Roos A. Left ventricular measurements with cine and spine-echo MR imaging: a study of reproducibility with variance component analysis. *Radiology* 1993;187:261–268.
3. Lorenz CH, Walker ES, Morgan VL, Klein SS, Graham TP Jr. Normal human right and left ventricular mass, systolic function, and gender differences by cine magnetic resonance imaging. *J Cardiovasc Magn Reson* 1999;1:7–12.
4. Kaji S, Yang PC, Kerr AB, Tang WHW, Meyer CH, Macovski AM, Pauly JM, Nisimura DG, Hu BS. Rapid evaluation of left ventricular volume and mass without breath-holding using real-time interactive cardiac magnetic resonance imaging system. *J Am Coll Cardiol* 2001;38: 527–33.
5. Hori Y, Yamada N, Higashi M, Hirai N, Nakatani S. Rapid evaluation of right and left ventricular function and mass using real-time true-FISP cine MR imaging without breath-hold: comparison with segmented true-FISP cine MR imaging with breath-hold. *J Cardiovasc Magn Reson*. 2003;5:439–50.
6. Schalla S, Klein C, Paetsch I, Lehmkuhl H, Bornstedt A, Schnackenburg B, Fleck E, Nagel E. Real-time MR image acquisition during high-dose dobutamine hydrochloride stress for detecting left ventricular wall-motion abnormalities in patients with coronary arterial disease. *Radiology* 2002;224:845–851.
7. Kellman P, Epstein FH, McVeigh ER. Adaptive sensitivity encoding incorporating temporal filtering (TSENSE). *Magn Reson Med* 2001;45:846–852.
8. Barkhausen J, Ruehm SG, Goyen M, Buck T, Laub G, Debatin JF. MR evaluation of ventricular function: true fast imaging with steady-state precession versus fast low-angle shot cine MR imaging: feasibility study. *Radiology* 2001;219:264–269.
9. Carr JC, Simonetti O, Bundy J, Li D, Pereles S, Finn JP. Cine MR angiography of the heart with segmented true fast imaging with steady-state precession. *Radiology* 2001;219:828–834.
10. Moon JC, Lorenz CH, Francis JM, Smith GC, Pennell DJ. Breath-hold FLASH and ISP cardiovascular MR imaging: left ventricular volume differences and reproducibility. *Radiology* 2002;223: 789–797.
11. Miller S, Simonetti OP, Carr J, Kramer U, Finn JP. MR imaging of the heart with cine true fast imaging with steady-state precession: influence of spatial and temporal resolutions on left ventricular functional parameters. *Radiology* 2002;223:263–269.
12. Yamamuro M, Tadamura E, Kubo S, Toyoda H, Nishina T, Ohba M, Hosokawa R, Kimura T, Tamaki N, Komeda M, Kita T, Konishi J. Cardiac functional analysis with multi-detector row CT and segmental reconstruction algorithm: comparison with echocardiography, SPECT, and MR imaging. *Radiology* 2005; 234:381–390.

13. Bland JM, Altman DG. Statistical methods for assessing agreement between two methods of clinical measurement. *Lancet* 1986;1:307–310.
14. Roussakis A, Baras P, Seimenis I, Andreou J, Danias PG. Relationship of number of phases per cardiac cycle and accuracy of measurement of left ventricular volumes, ejection fraction, and mass. *J Cardiovasc Magn Reson*. 2004;6:837–844.
15. Lee VS, Resnick D, Bundy JM, Simonetti OP, Lee P, Weinreb JC. Cardiac function : MR evaluation in one breath hold with real-time true first imaging with steady-state precession. *Radiology* 2002;222:835–842.
16. Barkhausen J, Goyen M, Ruhm SG, Eggebrecht H, Debatin JF, Ladd ME. Assessment of ventricular function with single breath-hold real-time steady-state free precession cine MR imaging. *Am J Rentgenol* 2002;178:731–735.
17. Plein S, Smith WH, Ridgway JP, Kassner A, Beacock DJ, Bloomer TN, Sivanathan MU. Qualitative and quantitative analysis of regional left ventricular wall dynamics using real-time magnetic resonance imaging: comparison with conventional breath-hold gradient echo acquisition in volunteers and patients. *J Magn Reson Imaging* 2001;14:23–30.
18. Wintersperger BJ, Nikolaou K, Dietrich O, Rieber J, Nittka M, Reiser MF, Schoenberg SO. Single breath-hold real-time cine MR imaging: improved temporal resolution using generalized autocalibrating partially parallel acquisition (GRAPPA) algorithm. *Eur Radiol* 2003;13:1931–1936.